



**HAL**  
open science

# A quasi steady state method for solving transient Darcy flow in complex 3D fractured networks accounting for matrix to fracture flow

B Noetinger

► **To cite this version:**

B Noetinger. A quasi steady state method for solving transient Darcy flow in complex 3D fractured networks accounting for matrix to fracture flow. *Journal of Computational Physics*, 2015, 283, pp.205 - 223. 10.1016/j.jcp.2014.11.038 . hal-01115492

**HAL Id: hal-01115492**

**<https://hal.science/hal-01115492>**

Submitted on 11 Feb 2015

**HAL** is a multi-disciplinary open access archive for the deposit and dissemination of scientific research documents, whether they are published or not. The documents may come from teaching and research institutions in France or abroad, or from public or private research centers.

L'archive ouverte pluridisciplinaire **HAL**, est destinée au dépôt et à la diffusion de documents scientifiques de niveau recherche, publiés ou non, émanant des établissements d'enseignement et de recherche français ou étrangers, des laboratoires publics ou privés.

1 A quasi steady state method for solving transient Darcy flow in complex 3D fractured  
2 networks accounting for matrix to fracture flow

3 B. Noëtinger\*

4 *IFP Energies nouvelles*

5 *1 & 4, avenue de Bois-Préau*

6 *92852 Rueil-Malmaison Cedex - France*

7 (Dated: August 8, 2014)

Modeling natural Discrete Fracture Networks (DFN) receives more and more attention in applied geosciences, from oil and gas industry, geothermal recovery. The fractures may be either natural, or artificial in case of well stimulation. Accounting for the flow inside the fracture network, and accounting for the transfers between the matrix and the fractures, with the same level of accuracy is an important issue for calibrating the wells architecture and for setting up optimal resources recovery strategies. Recently, we proposed an original method allowing to model transient pressure diffusion in the fracture network only. The matrix was assumed to be impervious. A systematic approximation scheme was built, allowing to model the initial DFN by a set of  $N$  unknowns located at the intersection between fractures. The higher  $N$ , the higher the accuracy of the model. The lowest order approximation  $N = 1$  appears under the form of solving a transient problem in a resistor/capacitor network, a so-called pipe network. Its topology is the same as the network of geometrical intersections between fractures.

In this paper, we generalize this approach in order to account for fluxes from matrix to fractures. We show that in the case of well separated time scales between matrix and fractures, the preceding model need only to be slightly modified in order to incorporate these fluxes. The additional knowledge of the so called matrix to fracture transfer function allows to modify the mass matrix that becomes a time convolution operator. This is reminiscent of existing space averaged transient dual porosity models.

Keywords: Flow in Fractured media, Discrete fracture network, Low permeability matrix, Quasi steady state, Dual porosity, Transfer function, Laplace transform

---

\*Electronic address: [benoit.noetinge@ifpen.fr](mailto:benoit.noetinge@ifpen.fr)

## 1. INTRODUCTION

Modeling of fluid flows including heat or chemical transfers into naturally fractured rocks using explicit descriptions of fractured media (DFN) is becoming increasingly popular among geoscientists. This growing interest is due to a wide range of applications in various industries, to a better characterization of fracture networks, and evidently to the increasing computing power. In the common practice, these detailed descriptions are used to build and to calibrate a so called “double porosity model” that is designed to manage field applications. This class of double porosity models corresponds to the large scale homogenized version of the Darcy equations in the fractured medium, coupled to a linear transfer model with the matrix that is acting as a reservoir. These models, which were proposed in the early 60’s by Barenblatt *et al* [2] remain still the base of most industrial fluid flow simulators [3–10]. Homogenization techniques [11–14], or Volume averaging techniques [15–17] allow a formal derivation of the double porosity equations, starting from the detailed DFN, at least in the Darcy hypothesis, and in the case of a well connected fracture network. Numerical solution of the associated closure problems permits to evaluate the parameters of the dual porosity model as a function of the geometry of the DFN. Useful connections with random walk theory providing efficient computational tools were made by several authors [18–22]. In the case of badly connected networks, modelling approaches involving percolation theory background are more appropriate [27–29]. But a complete workflow remains to be developed, especially if strong couplings with the matrix are involved, and in situations in which non linear transfers, like multiphase flow, are to be accounted for [8–10]. Direct simulations of flows in 2D or 3D DFN were already performed by several groups ([5, 30–40]). The underlying numerical methods involve finite volume, finite elements techniques. Some groups intend to couple the high resolution DFN model with a flow in the matrix [41].

Here, we focus on the simplest problem: fractures (here 2D objects like closed polygons or ellipses of small thickness  $\varepsilon$  of high typical conductivity  $C_f = k_f \times \varepsilon$  are embedded in a 3D matrix having a low permeability  $k_m \ll k_f$  that will be supposed as being uniform for sake of simplicity. The fractures are supposed to be well connected (FIG. 1). Our goal is to solve linear diffusion equation within such a medium. Considering large cases involving thousands of intersecting fractures, the main difficulty of direct numerical solution techniques is to get an automated meshing fulfilling the quality requirements of the associated discretization scheme [5, 40]. Even if this practical question is solved, the overall number of degrees of freedom remain equal to the number of fractures, say  $N$ , times the typical number of cells  $N_{typ}$  used to mesh every fracture (typically  $N_{typ} \simeq$  several hundred). The number of associated matrix elements should scale as  $N \times N_{typ}^{3/2}$ . Getting a numerical solution of a 10 millions fractures problem will imply thus solving close to several billion equations. This justifies developing approximation methods in which the number of degrees of

37 freedom remains close to the total number of connected intersections  $N_\cap$ . This was done in [1] assuming an impervious  
 38 matrix with  $k_m = 0$ . In that paper, it was shown that a systematic approximation scheme can be built that involves  
 39  $N_p$  unknowns that describe the trace of pressure at the intersections between fractures with increasing accuracy. At  
 40 first order,  $N_p = 1$ , which is equivalent to suppose that the pressure profiles at the intersection are uniform, the so  
 41 called pipe network model is recovered. The resulting equations possess the structure of a resistor/capacitor network  
 42 involving the total number of connected intersections  $N_\cap$ . The main physical assumption is that the considered time  
 43 scales are much more greater than a typical diffusion time over one single fracture. The resulting set of equations  
 44 reads:

$$\forall i = 1, N_\cap, m = 1, \infty, \quad \sum_{j \in J(i)} \sum_{n=1}^{\infty} K_{ij}^{mn} \times \frac{dP_j^n(t)}{dt} = \sum_{j \in J(i)} \sum_{n=1}^{\infty} T_{ij}^{mn} \times P_j^n. \quad (1)$$

45 Here, the integers  $i$  and  $j$  label the intersections,  $J(i)$  is the ensemble of the labels of intersections directly connected to  
 46 the  $i$ -th one. So as any intersection involves two different fractures, the set  $J(i)$  involves the whole set of intersections  
 47 belonging to both fractures intersecting at  $i$ . Labels  $m$  and  $n$  indicate the degrees of freedom corresponding to  
 48 the order of approximation of the pressure profiles at intersections.  $N_{\cap i}$  corresponds to all the other intersections  
 49 than  $i$  belonging to the pair of fractures the intersection of which is the  $i$  th intersection. The mass matrix  $\mathbf{K}$  and  
 50 the transmissivity matrix  $\mathbf{T}$  which are both symmetric positive can be related to  $L^2$  scalar products of elementary  
 51 mapping problems to be solved on each fracture domains independently of each other. In practice, truncating the  
 52 above equations with  $n = 1$  and  $m = 1$  corresponds to building a so called pipe network model characterized by  
 53 uniform pressure at the intersections. The model was successfully implemented for 3D DFN [42].

54 In the present paper, we generalize the method in order to account for the matrix to fracture flow. We show that  
 55 this can be achieved by changing the form of the mass term  $\sum_{j \in J(i)} \sum_{n=1}^{\infty} K_{ij}^{mn} \times \frac{dP_j^n(t)}{dt}$  under the form of a time  
 56 convolution involving the average transfer function  $f(t)$  between the matrix and the fracture:

$$\forall i = 1, N_\cap, m = 1, \infty, \quad \sum_{j \in J(i)} \sum_{n=1}^{\infty} K_{ij}^{mn} \times (V_f \delta(t) + V_m f(t)) * \frac{dP_j^n(t)}{dt} = \sum_{j \in J(i)} \sum_{n=1}^{\infty} V_f T_{ij}^{mn} \times P_j^n. \quad (2)$$

57 The  $*$  symbol corresponds to a time convolution.  $V_f$  and  $V_m$  represent the volumic fractions of the fractures and of  
 58 the matrix,  $V_f + V_m = 1$ . The transfer function  $f(t)$  [ $t^{-1}$ ] appears as a time variable porosity. This function can be  
 59 estimated by solving boundary value problem on the matrix blocks, or by alternative continuous time random walk

60 methods [20–22] that can avoid any explicit mesh of the matrix. Analytical forms  $f(t)$  accounting from both short  
 61 times and long times asymptotic behavior of  $f(t)$  can be proposed. Finally, the resulting equations 2 may be solved  
 62 in Laplace domain.

63 The paper is organized as follows: first, the Section 2 introduces the pressure diffusion model in the matrix and  
 64 in the fractures considered having a small thickness  $\varepsilon$ . In next Section 3.3.1, we summarize with more details the  
 65 techniques and results obtained in [1], that are also presented in more details in the appendices A,B,C. In section 4,  
 66 we present our assumptions to account for the matrix to fracture flow. In order to proceed, we must come back about  
 67 the mathematical treatment of the finite (not null) thickness of the fractures 4.4.1. We are thus in good position for  
 68 introducing the so called exchange function  $f(t)$  4.4.2 at the level of a single fracture. The explicit coupling of the  
 69 DFN to the matrix, as well as the adaptation of the projection formalism is presented in 4.4.3. Some general properties  
 70 of the exchange function are presented in section 5. In section 6, we come back about our main assumption of quasi  
 71 steady state flow inside the fractures, in order to check its consistency in the light of our findings. The application  
 72 of the formalism to the resistor capacitor network that will be employed in practice is given in 7, before giving some  
 73 comments and discussions.

## 74 2. MODEL PROBLEM, GEOMETRY AND NOTATIONS

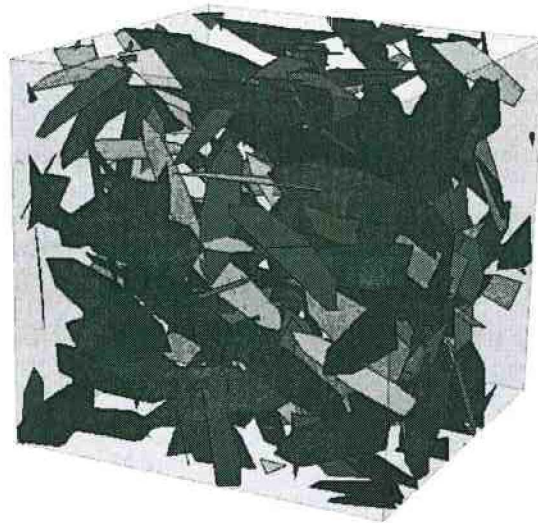


FIG. 1: 3D network of 2D polygonal fractures in a cubic box  $\Omega$ .

75 We consider flow in a 3D cubic domain  $\Omega$  containing  $N$  distinct permeable fractures (FIG. 1) embedded in a low  
 76 permeability matrix. No flux boundary conditions will be considered first at the frontier of  $\Omega$ . The individual  $I^{th}$

77 fracture is considered as being a closed 2D object (e.g. polygonal or elliptic), the position of which can be given by  
 78 the coordinates of its center, the orientation of its normal, and all the necessary parameters chosen by the geologist  
 79 to characterize its detailed shape.

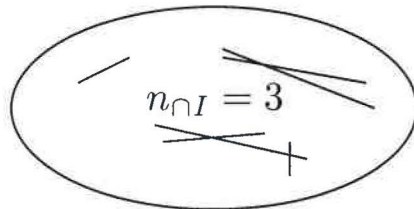


FIG. 2: An example of 2D elliptic fracture with a number of “cluster of intersections”  $n_{\cap I} = 3$ .

80 We consider a well connected network of  $N$  fractures, so each fracture is connected to all the others via at least one  
 81 path. So each fracture intersects at least one other fracture. Let  $n_{\cap I}$  denotes the number of disconnected cluster of  
 82 intersections of the  $I^{th}$  fracture with the others. By the name “cluster of intersections”, we mean that intersections  
 83 between different fractures can intersect between each other (see FIG. 2 ), providing clusters that are not necessarily  
 restricted as segments.

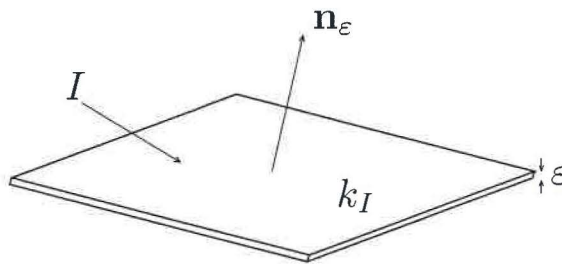


FIG. 3: 3D fracture of thickness  $\epsilon$  and of permeability  $k_I$ .

84  
 85 On the hydrodynamic point of view, we consider that all the fractures share a small common thickness denoted  
 86 by  $\epsilon$  (FIG. 3). The permeability of the  $I^{th}$  fracture is denoted by  $k_I$ . This permeability may vary on the fracture’s  
 87 plane, but in order to simplify notations, this dependence will not be explained, although it will be accounted for in  
 88 the  $\nabla$  operator manipulations.

89 Our main goal is to study the solution of the following diffusion problem when  $\epsilon$  is small of:

$$\varphi\mu c_t \frac{\partial p_{\epsilon}(\mathbf{r}, t)}{\partial t} = \nabla \cdot (k(\mathbf{r})\nabla p_{\epsilon}(\mathbf{r}, t)) + g(\mathbf{r}). \quad (3)$$

$$k(\mathbf{r}) = k_I \text{ if } \mathbf{r} \in \Omega_I \text{ for some } I = 1, \dots, N \quad (4)$$

$$k(\mathbf{r}) = k_m \text{ else} \quad (5)$$

90 The source term  $g(\mathbf{r})$  is arbitrary for the moment: it can be a bulk source term. Here, we do not have to add boundary  
 91 conditions at the fractures boundaries in contact with the matrix, but we may recall a normal flux continuity condition  
 92 that will be ensured :

$$(k_I \nabla p_\varepsilon(\mathbf{r}, t)) \cdot \mathbf{n}_\varepsilon = (k_m \nabla p_\varepsilon(\mathbf{r}, t)) \cdot \mathbf{n}_\varepsilon$$

93 We denote by  $D_f$  and  $D_m$  the associated diffusion coefficients.

$$D_f = \frac{k_I}{\varphi \mu c_t} \quad (6)$$

$$D_m = \frac{k_m}{\varphi \mu c_t} \quad (7)$$

$$D_m \ll D_f \quad (8)$$

94 Here  $\varphi$  is the porosity and  $c_t$  is the compressibility of the fluid, both are supposed to share the same value between  
 95 matrix and fractures, an hypothesis that can be easily relaxed.  $\mu$  is the fluid viscosity. Finally, in order to obtain a  
 96 well-posed evolution problem, we assume that initial value data at  $t = 0$  are provided.

### 97 3. THE PROJECTION FORMALISM

#### 98 3.1. The projection formalism in the case of an impervious matrix

99 In that section, we recall the results obtained in [1]. We consider first the steady state problem corresponding to  
 100 the long time limit of 3 with an impervious matrix  $k_m = 0$ . More details are given in the appendix A.

$$\nabla \cdot (k_I \nabla p_\varepsilon(\mathbf{r})) = g_I(\mathbf{r}),$$

101 The source term  $g_I(\mathbf{r})$  corresponds to the restriction of  $g(\mathbf{r})$  in the I th fracture domain. Notice that the Neumann'  
 102 boundary conditions at the frontier of  $\Omega$ , and the well connectivity of the network, give a perfectly well posed problem  
 103 in the fracture domain as far as the thickness  $\varepsilon$  is not equal to zero. In [1], it was shown that the solution of Laplace  
 104 equation in the fractured domain can be reconstructed once the trace of the pressure at the intersections between  
 105 fractures is known. These intersections are generally segments. This trace may be in turn decomposed by projection  
 106 on a complete set of basic function  $A$ . The n-th components of pressure on the j th intersection is denoted by  $P_j^n$ . In

107 order to determine  $P_j^n$ , one needs boundary conditions at every intersection. It was shown that a correct boundary  
 108 condition is that the sum of the (generally four) fluxes converging at a given point of the considered intersection is  
 109 equal to zero (see appendix A and [1]). Projecting thus this condition of the same set of basis function gives thus the  
 110 following linear system:

$$\forall i = 1, N_\Omega; m = 1, \infty, \sum_{j \in J(i)} \sum_{n=1}^{\infty} T_{ij}^{mn} \times P_j^n = B_i^m, \quad (9)$$

111 Explicit expressions for  $T_{ij}^{mn}$  are given in the appendix A. The right hand side  $B_i^m$  are linear forms involving the  
 112 source term  $g_I$  are also given in the same appendix.

### 113 3.2. Generalization to the transient case: the quasi steady state approximation

114 The projection formalism can be adapted in order to solve the transient diffusion equation 3 with a source term in  
 115 the fracture domain only. The proposed expression is a faithful approximation if the characteristic diffusion time over  
 116 one fracture (of typical value  $\tau \simeq \varphi \mu c_t L^2 / k_f \ll \tau_{g_I}$ ) is smaller than the characteristic time of variation of the source  
 117 term. this hypothesis is not restrictive at all and may be fulfilled in most practical cases. In that situation, the latter  
 118 can appear as being stationary. The net result is a generalization of 9 that reads:

$$\forall i = 1, N_\Omega; m = 1, \infty, \sum_{j \in J(i)} \sum_{n=1}^{\infty} K_{ij}^{mn} \times \frac{dP_j^n(t)}{dt} = \sum_{j \in J(i)} \sum_{n=1}^{\infty} T_{ij}^{mn} \times P_j^n + B_i^m. \quad (10)$$

119 The notations are essentially the same. This set of first order differential equations may be solved once an initial  
 120 condition is fulfilled.

121 Explicit evaluation methods of  $T_{ij}^{mn}$  and  $K_{ij}^{mn}$  are given in the appendix A and B. Both matrices  $\mathbf{K}$  and  $\mathbf{T}$  are  
 122 symmetric positive.

$$T_{ij}^{mn} = T_{ji}^{nm}, \quad (11)$$

$$K_{ij}^{mn} = K_{ji}^{nm}, \quad (12)$$

123 for all labels  $i, j, m$  and  $n$ .



## 4. INTRODUCING THE MATRIX TO FRACTURE FLOW

## 4.1. Basic assumptions, accounting for the finite thickness of the fractures

We are now in position to couple the fracture network with the matrix. In order to fix the ideas, we solve the initial value problem 3. The initial value data at  $t = 0$  is  $p(\mathbf{r}, \mathbf{t} = \mathbf{0}) = \mathbf{0}$  if  $\mathbf{r} \in \mathbf{matrix}$ . Our first assumption is to consider than the ratio of typical diffusion time over an elementary matrix block having a characteristic size of  $L$  (that can be considered as of the same order of magnitude of a fracture length) over a characteristic diffusion time over a single fracture that can be estimated as  $\frac{k_f}{k_m}$  is very large. So, the pressure inside the blocks can be considered as slowly varying in the time domain. This observation permits us to use the preceding projection formalism at quasi steady state. At a given time and at a given location  $\mathbf{r}$  inside a fracture, say the  $I$ -th fracture, one can compute a matrix to fracture flux  $f_{Imf}(\mathbf{r}, \mathbf{t})$  given by

$$f_{Imf}(\mathbf{r}, \mathbf{t}) = \frac{k_m}{\mu} (\nabla p_m^+(\mathbf{r}, \mathbf{t}) - \nabla p_m^-(\mathbf{r}, \mathbf{t})) \cdot \mathbf{n}_I \quad (13)$$

Here,  $\mathbf{n}_I$  is a vector normal to the  $I$  th fracture, and the  $+$  or  $-$  signs correspond to both sides of the fracture. At

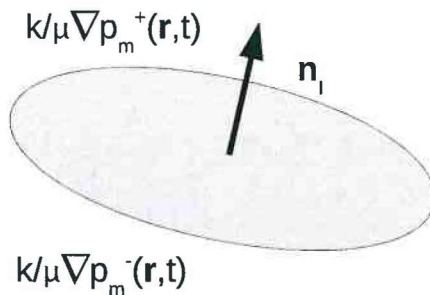


FIG. 4: Notations for the exchange flux

this stage, one must be careful with the small thickness  $\varepsilon$  of the fracture, by considering as an intermediate step the full 3D diffusion problem 3 involving both fracture and matrix. In order to get meaningful results, we impose that

137  $k_f \times \frac{|\Omega_f|}{|\Omega|} \gg k_m$ , that states that the overall permeability of the fracture network dominates the matrix permeability.  
 138 Since the fracture volume  $|\Omega_f|$  is proportional to the fracture thickness  $\varepsilon$ , the limit  $\varepsilon \rightarrow 0$  can causes some technical  
 139 difficulties. Keeping  $k_f$  constant and letting  $\varepsilon \rightarrow 0$  should lead to a vanishing influence of the fractures, that is not of  
 140 interest for our purposes. So, in the present situation in which we want to account for the matrix, it is more adapted  
 141 to consider that the overall fracture conductivity proportional to  $k_f \times \varepsilon$  is maintained fixed as  $\varepsilon$  tends to zero.  
 142 In order to decouple the fracture and matrix problems, one can integrate the local equation over the 3D volume  $V_\varepsilon$  of  
 143 thickness  $\varepsilon$  bounded by a surface  $\partial V_\varepsilon = S_\varepsilon \cup S_+ \cup S_-$ , as shown in FIG. 5. The surface  $S_\varepsilon$  is thus essentially a narrow  
 band of thickness  $\varepsilon$ . One obtains:

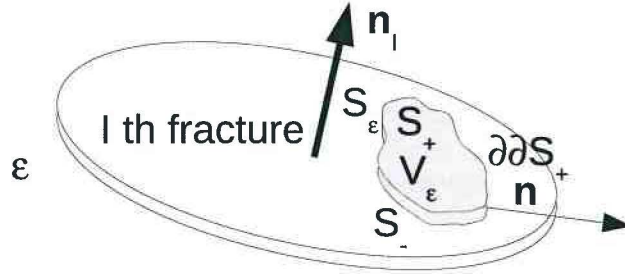


FIG. 5: Arbitrary integration domain  $V_\varepsilon$  over the I th fracture

144

$$\int_{V_\varepsilon} d^3(\mathbf{r}) \varphi \mu c_t \frac{\partial p_\varepsilon(\mathbf{r}, t)}{\partial t} = \int_{V_\varepsilon} d^3(\mathbf{r}) \nabla \cdot (k(\mathbf{r}) \nabla p_\varepsilon(\mathbf{r}, t)) \quad (14)$$

145 Using Green's theorem on the right hand side of this equation, one obtains:

$$\int_{V_\varepsilon} d^3 \mathbf{r} \varphi \mu c_t \frac{\partial p_\varepsilon(\mathbf{r}, t)}{\partial t} = \int_{\partial V_\varepsilon} d^2 \mathbf{r} \mathbf{n} \cdot (k(\mathbf{r}) \nabla p_\varepsilon(\mathbf{r}, t)) \quad (15)$$

146 So, using the decomposition  $\partial V_\varepsilon = S_\varepsilon \cup S_+ \cup S_-$ , one gets

$$\int_{V_\varepsilon} d^3\mathbf{r} \varphi \mu c_t \frac{\partial p_\varepsilon(\mathbf{r}, t)}{\partial t} = \int_{\partial S_\varepsilon} d^2\mathbf{r} \mathbf{n} \cdot (k(\mathbf{r}) \nabla p_\varepsilon(\mathbf{r}, t)) + \int_{\partial S_+} d^2\mathbf{r} f_{Imf}(\mathbf{r}, \mathbf{t}) \quad (16)$$

147 One can exploit the smallness of  $\varepsilon$  to estimate the various integrals and in order to decrease the order of integration.

$$\varepsilon \int_{S_+} d^2\mathbf{r} \varphi \mu c_t \frac{\partial p_\varepsilon(\mathbf{r}, t)}{\partial t} \simeq \varepsilon \int_{\partial \partial S_+} d\mathbf{r} \mathbf{n} \cdot (k(\mathbf{r}) \nabla p_\varepsilon(\mathbf{r}, t)) + \int_{\partial S_+} d^2\mathbf{r} f_{Imf}(\mathbf{r}, \mathbf{t}) \quad (17)$$

148 The  $2D$  integration was transformed into a  $1D$  one along the curve denoted by  $\partial \partial S_+$ . The normal vector  $\mathbf{n}$  is the  
 149 normal vector to the  $1D$  curve  $\partial \partial S_+$  belonging to the  $I$  th fracture plane. As the preceding equality is exact for any  
 150  $\partial \partial S_+$ , and using Green's theorem, one gets the local  $2D$  equation valid only on the fracture plane:

$$\varepsilon \varphi \mu c_t \frac{\partial p_\varepsilon(\mathbf{r}, t)}{\partial t} = \varepsilon \nabla \cdot (k(\mathbf{r}) \nabla p_\varepsilon(\mathbf{r}, t)) + f_{Imf}(\mathbf{r}, \mathbf{t}) \quad (18)$$

151 In present form, the limit  $\varepsilon \rightarrow 0$  can be evaluated safely. The differential operators are defined as in the preceding  
 152 sections on the considered fracture only. In practice, we have essentially to solve the same equations, up to a factor  
 153  $\varepsilon$ . The projection formalism can be used on the fracture domain using the following correspondence:

$$g_I(\mathbf{r}) = \frac{1}{\varepsilon} f_{Imf}(\mathbf{r}, \mathbf{t}) \quad (19)$$

154 The next issue will be to relate the interporosity flux  $f_{Imf}(\mathbf{r}, \mathbf{t})$  to the fracture pressure  $p_\varepsilon(\mathbf{r}, t) = p(\mathbf{r}, t)$ . The subscript  
 155  $\varepsilon$  can be suppressed now to simplify notations.

#### 156 4.2. About the matrix to fracture flow, the exchange function

157 In order to specify a workable form of  $f_{Imf}(\mathbf{r}, \mathbf{t})$ , a possible option is to relate  $f_{Imf}(\mathbf{r}, \mathbf{t})$  to the pressure map  $p_I(\mathbf{r}, \mathbf{t})$   
 158 of the  $I$  th fracture. The basic assumption is to consider a time convolution form that keeps the causality and linearity  
 159 of the underlying equations:

$$\frac{k_m}{\mu} \nabla p_m^+(\mathbf{r}, \mathbf{t}) \cdot \mathbf{n}_I = - \int_0^t dt' \mathbf{f}_{Im}^+(\mathbf{t} - \mathbf{t}') \frac{\partial \mathbf{p}_I(\mathbf{r}, \mathbf{t}')}{\partial \mathbf{t}'} \quad (20)$$

160 and so for the total source term accounting for both sides of the fracture:

$$g_I(\mathbf{r}) = -\frac{1}{\varepsilon} \int_0^t dt' f_{Im}(t-t') \frac{\partial p_I(\mathbf{r}, \mathbf{t}')}{\partial t'} \quad (21)$$

161 This form may be justified by the following arguments: let  $\Omega_m$  be a matrix block surrounded by several fractures.

162 Let  $P_f(t)$  be the pressure of these fractures, assumed to be spatially uniform. We consider a solution of the diffusion

163 equation inside the matrix block without any source term:

$$\varphi \mu c_t \frac{\partial p_m(\mathbf{r}, t)}{\partial t} = \nabla \cdot (k_m \nabla p_m(\mathbf{r}, t)) = 0, \quad (22)$$

$$p_m(\mathbf{r}, t) = P_f(t) \quad \text{if} \quad \mathbf{r} \in \partial\Omega_m \quad (23)$$

$$\forall \mathbf{r} \in \Omega_m, p_m(\mathbf{r}, t = 0) = 0$$

164 The present goal is to relate the flux  $\frac{k_m}{\mu} \nabla p_m^+(\mathbf{r}, \mathbf{t}) \cdot \mathbf{n}$ , or at least its average  $\frac{1}{|\partial\Omega_m|} \int_{\partial\Omega_m} d^2\mathbf{r} \frac{k_m}{\mu} \nabla p_m^+(\mathbf{r}, \mathbf{t}) \cdot \mathbf{n}$  to the

165 variations of the pressure at the boundary  $P_f(t)$ . Applying the divergence theorem, we obtain:

$$\int_{\partial\Omega_m} d^2\mathbf{r} \frac{k_m}{\mu} \nabla p_m^+(\mathbf{r}, \mathbf{t}) \cdot \mathbf{n} = -\varphi c_t |\Omega_m| \frac{d\langle P_m \rangle(t)}{dt} = -\varphi c_t \frac{d \int_{\Omega_m} d^3\mathbf{r} P_m(\mathbf{r}, \mathbf{t})}{dt}. \quad (24)$$

166 Here  $\langle \dots \rangle$  denotes a volume average of the pressure  $P_m$  over the matrix block. The minus sign comes from the normal

167  $\mathbf{n}$  orientation.

168 It is now possible to search for a relation between  $\langle P_m \rangle(t)$  and  $P_f(t)$  under the form of a convolution product:

$$\langle P_m \rangle(t) = \int_0^t dt' f(t-t') P_f(t'), \quad (25)$$

169 The mapping function  $f(t)$ , homogeneous to an inverse of time is the solution of a well posed boundary value problem

170 that will be discussed in more details in 5. Coming back to the average flux, using 24 and 25, and elementary

171 properties of convolution products, we get the following form:

$$\int_{\partial\Omega_m} d^2\mathbf{r} \frac{k_m}{\mu} \nabla p_m^+(\mathbf{r}, \mathbf{t}) \cdot \mathbf{n} = -\varphi c_t |\Omega_m| \int_0^t dt' f(t-t') \frac{dP_f(t')}{dt'},$$

172 Coming back to the local interporosity flux  $\frac{k_m}{\mu} \nabla p_m^+(\mathbf{r}, t) \cdot \mathbf{n}_I$  in the general case of a non uniform pressure in the  
 173 fractures, the preceding developments suggest the proposed form that leads to 21.

$$\frac{k_m}{\mu} \nabla p_m^+(\mathbf{r}, t) \cdot \mathbf{n}_I = - \int_0^t dt' \varphi c_t \frac{|\Omega_m|}{|\partial\Omega_m|} \mathbf{f}^+(\mathbf{t} - \mathbf{t}') \frac{\partial p_I(\mathbf{r}, \mathbf{t}')}{\partial t'} \quad (26)$$

174 The subscript + recalls that any location in a fracture is in contact with two matrix blocks. Adding both contri-  
 175 butions, we get:

$$g_I(\mathbf{r}) = -\varphi c_t \frac{|\Omega_m|}{\varepsilon |\partial\Omega_m|} \int_0^t dt' f(t-t') \frac{\partial p_I(\mathbf{r}, \mathbf{t}')}{\partial t'} \quad (27)$$

$$= -\varphi c_t \frac{V_m}{V_f} \int_0^t dt' f(t-t') \frac{\partial p_I(\mathbf{r}, \mathbf{t}')}{\partial t'} \quad (28)$$

176 A more detailed discussion about the  $f(t)$  functions will be provided in section 5. We now turn our attention about  
 177 the final closure of the problem, and the resulting consequences on the projection formalism.

### 178 4.3. Final closure and projection formalism

179 Combining 3 and 28, we get an equation driving  $p(\mathbf{r}, t)$  inside any fracture:

$$\varphi \mu c_t \frac{\partial p(\mathbf{r}, t)}{\partial t} = \nabla \cdot (k_I \nabla p(\mathbf{r}, t)) - \frac{V_m}{V_f} \varphi \mu c_t \int_0^t dt' f(t-t') \frac{\partial p(\mathbf{r}, \mathbf{t}')}{\partial t'}$$

180 When it is possible, we suppress the subscript  $I$  because we are considering local pressure without any ambiguity on  
 181 the  $I$  th fracture. As the local pressure  $p(\mathbf{r}, t)$  appears in both members, the original diffusion equation becomes an  
 182 integral equation which can be rewritten under the alternative form:

$$\int_0^t dt' \varphi \mu c_t (V_f \delta(t-t') + V_m f(t-t')) \frac{\partial p(\mathbf{r}, \mathbf{t}')}{\partial t'} = V_f \nabla \cdot (k_I \nabla p(\mathbf{r}, t))$$

183 As in [1], we introduce the following pressure decomposition, see appendices A and B for the details.

$$p(\mathbf{r}, t) = \delta p(\mathbf{r}, t) + \sum_{j \in J_I} \sum_{n=1}^{\infty} P_j^n(t) \hat{P}_j^n(\mathbf{r})$$

184 The pressure fluctuation  $\delta p(\mathbf{r}, t)$  follows the equation:

$$\begin{aligned} \varphi \mu c_t \int_0^t dt' (V_f \delta(t-t') + V_m f(t-t')) \frac{\partial \delta p(\mathbf{r}, t')}{\partial t} &= V_f \nabla \cdot (k_I \nabla \delta p(\mathbf{r}, t)) \\ &- \sum_{j \in J_I} \sum_{n=1}^{\infty} \int_0^t \varphi \mu c_t (V_f \delta(t-t') + V_m f(t-t')) \dot{P}_j^n(t') \hat{P}_j^n(\mathbf{r}), \end{aligned} \quad (29)$$

185 with an additional condition:

$$\delta p(\mathbf{r}, t) = 0 \quad \text{if } \mathbf{r} \in \cup \cap_i.$$

186 Here, the  $P_j^n(t)$  are assumed to be “slowly varying” if compared to typical diffusion time over one fracture. The  
187 steady state assumption assumes that the residual term  $\delta p(\mathbf{r}, t)$  obeys a steady state equation in which the left hand  
188 side is considered as negligible. The validity of this major assumption will be discussed in more details in section 6.

189 So, we assume that

$$V_f \nabla \cdot (k_I \nabla \delta p(\mathbf{r}, t)) = \sum_{j \in J_I} \sum_{n=1}^{\infty} \int_0^t \varphi \mu c_t (V_f \delta(t-t') + V_m f(t-t')) \dot{P}_j^n(t') \hat{P}_j^n(\mathbf{r}),$$

190 We can combine B2 and 19 to get:

$$\forall i, m, \quad \sum_{j \in J(i)} \sum_{n=1}^{\infty} K_{ij}^{mn} \times \int_0^t (V_f \delta(t-t') + V_m f(t-t')) \frac{dP_j^n(t')}{dt} = \sum_{j \in J(i)} \sum_{n=1}^{\infty} V_f T_{ij}^{mn} \times P_j^n \quad (31)$$

191 This is the proposed equation 2. Further insights can be given introducing time domain Laplace transform defined  
192 by

$$g(s) = \int_0^{\infty} \exp - st g(t) dt \quad (32)$$

193 With the property for the Laplace transform of the time derivative of a function  $g(t)$ :

$$\left[\frac{dg(t)}{dt}\right](s) = sg(s) - g(t=0) \quad (33)$$

194 By convention, throughout the rest of the paper, employing a  $s$  argument corresponds to using the Laplace transform  
195 of any function  $g(t)$ .

196 The Laplace transform of 31 gives :

$$\forall i, m, \quad \sum_{j \in J(i)} \sum_{n=1}^{\infty} K_{ij}^{mn} \times (V_f + V_m f(s)(sP_j^n(s) - P_j^n(t=0))) = \sum_{j \in J(i)} \sum_{n=1}^{\infty} V_f T_{ij}^{mn} \times P_j^n(s) \quad (34)$$

197 In the Laplace domain, the net effect of the matrix is a modification of the porosity by a  $s$  dependent porosity.  
198 Setting  $V_m = 0$ , one recovers the impervious matrix case equations 1. It appears that having a solution of the  
199 corresponding impervious matrix problem given by 1 using Laplace transforms, and replacing the Laplace argument  
200  $s$  by  $s(V_f + V_m f(s))$  will provide the solution of 34. Numerical Laplace inversion can be performed with accuracy  
201 by Stehfest algorithm [45]. The net result is that using Laplace transform techniques, the additional computational  
202 cost relies mainly in the determination of the exchange function  $f(\cdot)$ . This observation was already highlighted by  
203 several authors in the context of the averaged continuous double porosity descriptions with transient interporosity  
204 flow [24–26].

205 Finally, for small  $s$ , as  $f(s) \sim 1$  (section 5) corresponding to long time relaxation or low frequencies forcing, one  
206 obtains, coming back to the time domain:

$$\forall i, m, \quad \sum_{j \in J(i)} \sum_{n=1}^{\infty} K_{ij}^{mn} \frac{dP_j^n}{dt} \simeq \sum_{j \in J(i)} \sum_{n=1}^{\infty} V_f T_{ij}^{mn} \times P_j^n(t) \quad (35)$$

207 This corresponds to the original set of equations, up to a  $V_f$  factor that appears as a retention factor that will hinder  
208 diffusion in the fracture domain.

## 5. ABOUT THE EXCHANGE FUNCTION

### 5.1. Numerical evaluation of the exchange function

We can now study the exchange function as well as its practical evaluation. We recall 25 relating the volume average  $\langle P_m \rangle(t)$  = of the pressure in the matrix to the forcing imposed by the boundary condition in the fractures  $P_f(t)$ :

$$\langle P_m \rangle(t) = \int_0^t dt' f(t-t') P_f(t'),$$

Or, equivalently using Laplace transforms:

$$\langle P_m \rangle(s) = f(s) P_f(s) \tag{36}$$

Choosing as  $P_f(t)$  a Heaviside function gives:  $\langle P_{Hm} \rangle(t) = \int_0^t dt' f(t')$ , from which  $f(t)$  can be obtained by direct time derivative evaluation. So, solving the following boundary value problem:

$$\varphi \mu c_t \frac{\partial p_{Hm}(\mathbf{r}, t)}{\partial t} = \nabla \cdot (k_m \nabla \delta p_{Hm}(\mathbf{r}, t)), \tag{37}$$

$$p_m(\mathbf{r}, t) = 1 \quad \text{if } \mathbf{r} \in \partial \Omega_m, t > 0 \tag{38}$$

$$p_m(\mathbf{r}, t = 0) = 0 \quad \forall \mathbf{r} \in \Omega_m \tag{39}$$

and computing the average  $\langle P_{Hm} \rangle(t)$  yields the exchange function. This evolution equation can be solved by several numerical methods. The main task is to mesh the matrix. Note that any explicit meshing of the fractures is avoided because the fractures enter only via a Dirichlet boundary condition. The resulting linear systems to be solved will not contain highly contrasted coefficients, because  $k_f$  does not enter in the problem, so correct preconditioning properties can be expected. A useful alternative interpretation of the exchange function in terms of random walks can be proposed [20, 22]. Alternative numerical techniques such as MINC approaches can also be employed [37].

### 5.2. Properties of the exchange function

Equations 25 and 39 permits to obtain some analytical solutions in simple cases for  $f(t)$  or  $f(s)$ . We can consider 1D blocks (the associated coordinate  $x \in [0, 2\ell]$  perpendicular to the plane of the fracture). The potential  $p_{Hm}(x, t)$



225 depends on  $x$  and  $t$ , So one can use the 1D solution:

$$\begin{aligned} \frac{\partial p_{Hm}(x, t)}{\partial t} &= D_m \frac{\partial^2 p_{Hm}(x, t)}{\partial x^2}, & (40) \\ p_m(x = 0, t) &= 1 \text{ for } t > 0 \\ \frac{\partial p_{Hm}}{\partial x}(x = \ell, t) &= 0, \text{ for } t > 0 \text{ by symmetry} \\ \forall x \neq 0, p_m(x, t = 0) &= 0 \end{aligned}$$

226 this equation can be solved using time domain Laplace transform:

$$\begin{aligned} sp_{Hm}(x, s) &= D_m \frac{\partial^2 p_{Hm}(x, s)}{\partial x^2}, & (41) \\ p_m(x = 0, s) &= 1/s \\ \frac{\partial p_{Hm}}{\partial x}(x = \ell, s) &= 0, \text{ for } t > 0 \text{ by symmetry} & (42) \end{aligned}$$

227 This single variable differential equation can be solved easily. One obtains finally:

$$f(s) = \frac{\sqrt{D_m}}{\ell\sqrt{s}} \times th\left(\sqrt{\frac{s}{D_m}}\ell\right) \quad (43)$$

228 At short times  $t$ , when the potential in the fractures corresponding to the boundaries of the matrix blocks, is set to  
 229 1, the diffusion in the matrix takes place only in a small boundary layer close to the fractures. One can adopt two  
 230 point of views, in the first one, one can write  $f(s) = \frac{\sqrt{D_m}}{\ell\sqrt{s}} \times th\left(\sqrt{\frac{s}{D_m}}\ell\right) \simeq \frac{\sqrt{D_m}}{\ell\sqrt{s}}$ . In the second point of view, one  
 231 can consider that the matrix blocks are infinite,  $\ell = \infty$ , which does not permit using 43 directly because the average  
 232 pressure on the matrix is not well defined. But, one can use directly the evaluation 20 of the matrix to fracture flux.

$$\begin{aligned} sp_{Hm}(x, s) &= D_m \frac{\partial^2 p_{Hm}(x, s)}{\partial x^2}, & (44) \\ p_m(x = 0, s) &= 1/s \end{aligned}$$

233 and to compute  $\varphi c_t D_m \frac{\partial p(H_m)}{\partial x}(x=0, s)$  for  $x > 0$  by symmetry to obtain:

$$f(s) = \frac{\sqrt{D_m}}{\sqrt{s}} \times \frac{|\partial \Omega_m|}{|\Omega_m|} \quad (45)$$

234 In the real time domain, this corresponds to

$$f(t) = \frac{\sqrt{D_m}}{\sqrt{\pi} \sqrt{t}} \times \frac{|\partial \Omega_m|}{|\Omega_m|} \quad (46)$$

235 Comparing both results shows that for consistency,  $\ell = \frac{|\Omega_m|}{|\partial \Omega_m|}$ . This formula can be interpreted as follows: at short  
236 times  $t$ , the characteristic diffusion length is of the order of  $\sqrt{D_m t}$ . So the corresponding flux is given by 46 up to  
237 numerical constants. This corresponds to the large  $s$  asymptotics of  $f(s)$ .

238 Several other general properties of  $f(t)$  can be attained by studying the limit  $s \rightarrow 0$ . One has, using a Taylor  
239 expansion of the  $th$  function:

$$f(s) = 1 - \frac{1}{3} \frac{s}{D_m} \ell^2 + \dots \quad (47)$$

240 We observe that  $f(s=0) = 1$ . This is a general equality that occurs because using 36 and remarking that both  
241 fracture and matrix potential equalize at the long times (or low frequency) limit so  $f(s=0) = 1$ . In next paragraph,  
242 we show that the linear term in  $s$  is closely related to the so called "exchange coefficient"  $\alpha_\infty = 3 \frac{D_m}{V_m \ell^2}$  in present case.  
243 This coefficient arises from large scale averaging theories that yields homogenized form of double porosity equations  
244 [21] valid at long times, long distances. A useful interpretation of  $f(t)$  in terms of escape time pdf from the matrix  
245 was derived in [20, 22]. It corresponds to the exit time distribution from the matrix blocks of a particle undergoing  
246 brownian motion of diffusion coefficient  $\frac{k_m}{\phi \mu c_t}$ . In particular, the average exit time may be directly related to the so  
247 called exchange coefficient or "shape factor" that enter in classical dual porosity models [17, 21]. Continuous time  
248 random walk techniques can thus be set-up to determine this exit time distribution. This can provide techniques  
249 avoiding any explicit meshing of the matrix. Detailed expressions of exchange functions using Laplace transforms are  
250 given for several block geometries by de Swann [23–25], that can be useful for testing numerical solutions or analytical  
251 parameterizations.

### 5.3. The steady state double porosity case

252

253 It can be shown that choosing the following form for  $f(s)$

$$f(s) \approx \frac{\alpha_\infty}{V_m s + \alpha_\infty} \quad (48)$$

254 corresponding to an exponential relaxation in the time domain is equivalent to consider a steady state double porosity  
255 model [22]. Using 48 and 24, it is possible to show that at a given time, the flux between matrix and the fractures is  
256 given by:

$$\frac{k_m}{\mu} \nabla p_m(\mathbf{r}, \mathbf{t}) \cdot \mathbf{n} = \frac{|\Omega_m|}{|\partial\Omega_m|} \varphi c_t \alpha_\infty (\langle \mathbf{P}_m \rangle(\mathbf{t}) - \mathbf{P}_I(\mathbf{t})) \quad (49)$$

257 This corresponds to a steady state double porosity model with a particular choice of the so called shape factor  $\alpha_\infty$   
258 [17]. The flux is proportional to the difference between the pressure of the matrix and the fracture. The reader should  
259 note that in [22], the exchange function  $f(s)$  corresponds to  $V_f + V_m f(s)$ .

260

## 6. TESTING THE SELF CONSISTENCY OF THE ASSUMPTIONS

261 In that section, we verify on a simplified test problem whether the quasi steady state assumption of section 4.4.3 is  
262 consistent with the subsequent findings. In other words, we check if the source term arising from the matrix does not  
263 modify drastically the pressure diffusion inside a fracture, that could lead to fracture relaxation time comparable with  
264 the matrix relaxation time. We come back about a simplified form of 30 on a single fracture, keeping our notations:

$$\varphi \mu c_t \int_0^t dt' (V_f \delta(t-t') + V_m f(t-t')) \frac{\partial \delta p(\mathbf{r}, t')}{\partial t} = V_f \nabla \cdot (k_I \nabla \delta p(\mathbf{r}, t)) \quad (50)$$

$$\delta p(\mathbf{r}, t = 0) \quad \text{fixed}$$

265 It corresponds to an initial value problem on the fracture domain, without source term. We want to check if the  
266 relaxation time associated with the operator  $\varphi \mu c_t \int_0^t dt' (V_f \delta(t-t') + V_m f(t-t')) \frac{\partial \delta p(\mathbf{r}, t')}{\partial t}$  is small compared with the  
267 diffusion time in the matrix  $\simeq D_m / \ell^2$ . In order to proceed, we consider that  $f(s)$  is given by the steady state double  
268 porosity model 48. We replace also the Laplace operator  $V_f \nabla \cdot (k_I \nabla \delta p(\mathbf{r}, t))$  by its smallest eigenvalue corresponding to  
269 the larger relaxation time of the fracture:  $V_f \nabla \cdot (k_I \nabla \delta p(\mathbf{r}, t)) \sim -V_f \varphi \mu c_t \lambda \delta p(\mathbf{r}, t)$ . Here,  $\lambda \sim D_f / \ell^2 \gg \alpha_\infty \sim D_m / \ell^2$ .

270 The negative sign was chosen to recall that the Laplace operator has negative eigenvalues. Using Laplace transform,  
 271 and the property 33, we get:

$$(V_f + V_m \frac{\alpha_\infty}{V_m s + \alpha_\infty}) s \delta p(\mathbf{r}, s) = -V_f \lambda \delta p(\mathbf{r}, s) + V_f \delta p(\mathbf{r}, t = 0)$$

272 or, equivalently:

$$\delta p(\mathbf{r}, s) = \frac{(V_m s + \alpha_\infty)}{(V_f V_m s^2 + (\alpha_\infty + \lambda V_f V_m) s + V_f \lambda \alpha)} V_f \delta p(\mathbf{r}, t = 0)$$

273 Recalling the boundary conditions for  $\delta p(\mathbf{r}, s) = 0$  at the fractures intersections, it is clear that for large time  
 274  $\delta p(\mathbf{r}, t) \rightarrow 0$  for  $t \rightarrow \infty$ . The convergence is exponential and in order to estimate the relaxation time, the roots of  
 275 the denominator has to be evaluated. The resulting expressions can be simplified using the fact that  $\alpha_\infty \ll \lambda$ , and  
 276 we obtain two roots, up to terms of order  $\frac{\alpha_\infty}{\lambda} \ll 1$ , which are  $-\lambda$  and  $-\frac{\alpha_\infty}{\varphi_m}$ . Finally, after simplification with the  
 277 numerator, we get:

$$\delta p(\mathbf{r}, s) = \frac{1}{s + \lambda} \delta p(\mathbf{r}, t = 0)$$

278 equivalent to:

$$\delta p(\mathbf{r}, t) = \exp - (\lambda t) \delta p(\mathbf{r}, t = 0)$$

279 This confirms the fast relaxation of the transient and the justification of the quasi steady state approximation.

## 280 7. APPLICATION TO THE RESISTOR CAPACITOR, OR PIPE NETWORK

281 In that subsection, we restrict the problem to the case  $m = 1$  and  $n = 1$  used in practice [42]. In practice it means  
 282 physically that we estimate only the average pressure along each intersection, and that the mass conservation equation  
 283 at the intersection is only fulfilled globally. Assuming that all  $P_i^m = 0$  if  $m \geq 2$ , the differential system to be solved  
 284 is:

$$\forall i, \quad \sum_{j \in J(i)} K_{ij}^{11} \times (V_f \delta(t) + V_m f(t)) * \frac{dP_j^1(t)}{dt} = \sum_{j \in J(i)} V_f T_{ij}^{11} \times P_j^1. \quad (51)$$

285 We recall the following relation [1]:

$$\sum_{ij \in \Omega_I} K_{ij}^{11} = \varphi \mu c_t \int_{\Omega_I} d^2 \mathbf{r} = \varphi \mu c_t S_I,$$

286 where  $S_I$  is the total area of the fracture.

287 The resulting time discretization scheme of the differential equations (51) can be rather time consuming in the  
 288 case of large fracture networks. It is thus appealing to use a mass condensation (or mass lumping) scheme by  
 289 acknowledging that pressure variations of neighboring nodes will be very close together. We replace  $\sum_{j \in J(i)} K_{ij}^{11} \times$   
 290  $\frac{dP_j^1(t)}{dt}$  by  $\sum_{j \in J(i)} K_{ij}^{11} \times \frac{dP_i^1(t)}{dt}$ . So we get:

$$\forall i, \quad M_i \times (V_f \delta(t) + V_m f(t)) * \frac{dP_i^1(t)}{dt} = \sum_{j \in J(i)} V_f T_{ij}^{11} \times (P_j^1 - P_i^1), \quad (52)$$

$$\text{with } M_i = \sum_{j \in J(i)} K_{ij}^{11}. \quad (53)$$

291 Indeed, these equations (52) possess the structure of the equations driving the variations of the node potentials of  
 292 a resistor/capacitor network. The main difference is that the capacity term appears under the form of convolution  
 293 products, that are simple products in the Laplace domain.

294 The numerical determination of the  $T_{ij}^{11}$  can be done by solving  $n_n$  elementary Laplace problems with the boundary  
 295 conditions at the intersections, and computing next the scalar products (A15). Thus, the masses  $M_i$  given by (53)  
 296 are obtained using a suitable surface integration scheme. Fast evaluations of these quantities avoiding solving local  
 297 Laplace problems on each fracture are proposed in [42].

## 298 8. FINAL COMMENTS AND DISCUSSIONS

299 In this paper, we generalize a method that permits to solve diffusion problems in complex 3D fracture networks  
 300 using a relatively small number of degrees of freedom. The generalization enables us to consider flows coupled with a  
 301 low permeability matrix acting as a reservoir. The flow exchanges with the matrix can be modeled using the so called

302 exchange function  $f(\cdot)$ . The main assumption is that diffusion is so fast in the fractures that the matrix blocks are  
 303 bounded by essentially spatially uniform boundary conditions that are quasi steady state. The second assumption  
 304 is to replace the local matrix to fracture flux by its average. Both assumptions permit to define  $f(\cdot)$  as a volume  
 305 average of a solution of a well posed boundary value problem. This function can be determined by existing numerical  
 306 techniques that avoid a complex meshing of the DFN and solving a badly conditioned problem. It posses also a  
 307 probabilistic interpretation as it represents the pdf of escape time of diffusing particle in the matrix. Alternatively, it  
 308 can be parameterised using generic analytical forms fulfilling asymptotic requirements at short and long times. These  
 309 forms permit to capture the essential features of the matrix: The surface to volume ratio, the typical size  $L$  of the  
 310 blocks, and a shape factor. Very ramified DFN with many dead ends having fractal like structures could be described  
 311 using a power law  $f(\cdot)$  function accounting for scale dependent surface to volume ratio. Using Laplace transform  
 312 techniques, we show that the effect of the matrix can be modeled at a small extra cost once a previous modeling  
 313 of potential diffusion in the DFN with an impervious matrix is available. No major extra computing cost can be  
 314 expected. Numerical tests have to be carried out in order to test the accuracy of the approach, and especially of the  
 315 limitation to the pipe network approximation ( $n, m$ ) restricted to 1. Another issue is the generalization of the present  
 316 formalism to other transport equations, such as convection diffusion equations in the fracture network, coupled with  
 317 purely diffusive transport in the matrix. This could be done following works of [27] and [28].

## 318 APPENDIX A: PROJECTION FORMALISM STEADY STATE CASE

### 319 1. Small fracture thickness limit

320 The projection method follows several steps. The first one is to account for the small thickness  $\varepsilon$  of the fractures in  
 321 order to be able to treat the intersection between fractures as  $1D$  objects, and the fractures as  $2D$  objects embedded  
 322 in a  $3D$ .

323 Some geometrical quantities and several notations are presented in (FIG. 6). Let  $\cap_{IJ}$  be an intersection between  
 324 the two fractures  $I$  and  $J$ ; a  $3D$  volume having the shape of a match. As  $\varepsilon$  tends to zero, this volume becomes a  
 325  $1D$  segment corresponding to the intersection of the two planes containing fractures  $I$  and  $J$ . In order to simplify  
 326 the discussion, and this changes nothing to the global solution, we consider that this segment does not intersect a  
 327 third fracture. Let  $x$  denote a coordinate along this segment. The point  $\mathbf{r}_{\cap_{IJ}}(x)$  denotes in a rather natural way the  
 328 generic point of this segment labeled by  $x$  (in practice, the three coordinates of  $\mathbf{r}_{\cap_{IJ}}(x)$  may depend linearly on  $x$ ).

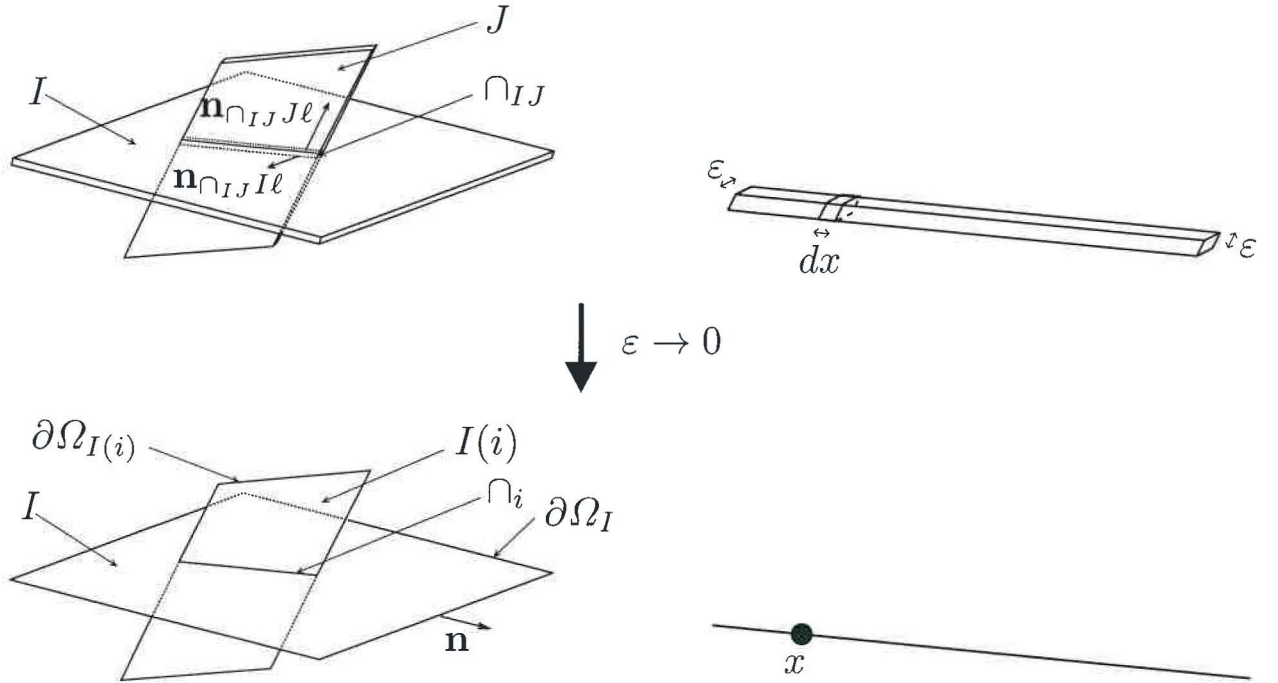


FIG. 6: Geometry and notation two rectangular fractures and the associated intersection, and limit  $\varepsilon \rightarrow 0$ .

329 As  $\varepsilon$  tends to zero, we can consider that close to the point  $\mathbf{r}_{\cap_{IJ}}(x)$ , the intersection separates locally the  $I^{th}$  fracture  
 330 (resp  $J^{th}$ ) in two halves denoted arbitrary by the suffix  $\ell$  and  $r$  (for left and right). We introduce also the normal  
 331  $\mathbf{n}_{\cap_{IJ}I\ell}$  as being the normal to intersection  $\cap_{IJ}$  pertaining to the plane of the  $I^{th}$  fracture, pointing in the  $\ell$  direction.  
 332 In addition, it is possible to introduce the  $\nabla_I$  gradient operator as being the  $2D$  gradient operator operating only in  
 333 the  $I^{th}$  fracture plane. When there is no ambiguity, we will remove the index  $I$  to this operator.

334 We denote the considered limit as  $\lim_{\varepsilon \rightarrow 0}(p_\varepsilon(\mathbf{r})) = p(\mathbf{r})$ . We argue that  $p(\mathbf{r})$  is the solution of the following problem:

$$\forall I = 1, \dots, N, \quad \nabla_I \cdot (k_I \nabla_I p(\mathbf{r})) = g_I(\mathbf{r}). \quad (\text{A1})$$

335 The notation  $\nabla_I \dots$  corresponds to the  $2D$  gradient operator defined in the fracture. In order to get a meaningful limit,  
 336 we must specify boundary conditions at the frontiers of the computational domain, at the boundary of each fracture,  
 337 and finally at the intersections between fractures.

338 The boundary condition at the frontier  $\Omega$  of the computational domain remains essentially unchanged (notice that  
 339 the same reasoning should hold also when using mixed Dirichlet Neumann conditions). Considering now each fracture,  
 340 the boundary value problem to be solved is  $2D$ . The position vector  $\mathbf{r}$  is essentially  $2D$ . In particular, the boundary  
 341 condition at the border of each fracture, say  $\partial\Omega_I$  in the  $I^{th}$  fracture plane, (a  $1D$  curve, corresponding for example

342 to an ellipse in the case of elliptic fractures) can be written as:

$$k_I \nabla p(\mathbf{r}) \cdot \mathbf{n} = 0,$$

343 where  $\mathbf{n}$  is the outward normal to the boundary (FIG. 6). Notice that in the present formulation, the two initial faces  
344 of the fracture in direct contact with the matrix do not play any role.

345 In order to get a well-defined problem, a boundary condition must be specified at every intersection between  
346 fractures. In [1], the following condition was proposed:

$$\mathbf{n}_{\cap_{IJ}\ell} \cdot k_I [\nabla_I p(\mathbf{r}_{\cap_{IJ}}(x))_\ell - \nabla_I p(\mathbf{r}_{\cap_{IJ}}(x))_r] + \mathbf{n}_{\cap_{IJ}r} \cdot k_J [\nabla_J p(\mathbf{r}_{\cap_{IJ}}(x))_\ell - \nabla_J p(\mathbf{r}_{\cap_{IJ}}(x))_r] = 0. \quad (\text{A2})$$

347 It means physically that at each location of the intersection, the four fluxes converging at the considered position  
348 must balance. The subscript  $\ell$  and  $r$  (left and right) account for the two sides of the intersection. The normal  $\mathbf{n}_{\cap_{IJ}}$   
349 is one normal vector to the intersection under consideration lying in the plane of the  $I$  th fracture involved in the  
350 intersection. This condition reflects that due to the small transverse area of the intersection, longitudinal flow in the  
351 intersection will become negligible as  $\varepsilon \rightarrow 0$ , independently on the value of permeability value at the intersection.  
352 Note that the same argument can be followed in the case of a transient problem, because the volume integral of the  
353 accumulation term inside the intersection will also become negligible.

## 354 2. The projection method.

355 We are in position to build an approximation scheme allowing us to eliminate internal degrees of freedom inside  
356 each fracture. In a finite element solution framework, using an explicit mesh of each fracture, these degrees of freedom  
357 will correspond to the unknowns associated with the generic element inside each fracture. The basic idea is to express  
358 these lumped degrees of freedom as a function of the pressure trace at intersections. Thus, using the boundary  
359 condition (A2), we get equations coupling only degrees of freedom attached to intersections. In order to proceed, we  
360 focus our attention over the  $I^{th}$  fracture called  $\Omega_I$  of the set. In order to simplify the analysis, we suppose that this  
361 fracture intersects  $n_{\cap I}$  other fractures by simple intersections restricted to be segments. So, the  $n_{\cap I}$  intersections are  
362 non-intersecting segments denoted by  $\cap_j$  of arbitrary lengths, the label of which belong to a subset of the  $N_{\cap}$  labels  
363 denoted  $J_I$ , such that  $Card J_I = n_{\cap I}$ . For the intersection labeled by  $i$ , we call  $I(i)$  the label of the other fracture



364 that is intercepted by  $I$  (FIG. 6). So we have  $J(i) = J_I \cup J_I(i)$ . By hypothesis, this fracture is well defined.

365 For each intersection segment, we introduce a complete set of basis functions, denoted by  $\Phi_j^n(x)$ . Here, the integer  
366  $n = 1, \dots, \infty$  labels the function, while  $j = 1, \dots, n_{\cap I}$  labels the intersection number. We add two conditions:

$$\Phi_j^1(x) = 1, \quad (\text{A3})$$

$$\int_{\cap_j} \Phi_j^n(x) dx = 0 \quad \text{if } n \geq 2. \quad (\text{A4})$$

367 Possible choices could involve sine and cosine functions, or polynomial families like Legendre or Tchebychev. Notice  
368 that up to a dilatation due to the varying length of the intersection, the same set of functions can be retained for every  
369 intersection between any fractures. We introduce elementary solutions defined by  $\hat{P}_j^n(\mathbf{r})$ , solution of the following  
370 boundary value problem:

$$\begin{cases} \nabla_I \cdot (k_I \nabla \hat{P}_j^n(\mathbf{r})) = 0, \\ k_I \nabla \hat{P}_j^n(\mathbf{r}) \cdot \mathbf{n} = \mathbf{0} \quad \text{on } \partial\Omega_I, \\ \hat{P}_j^n(\mathbf{r}) = \delta_{ij} \times \Phi_j^n(\mathbf{r}) \quad \text{if } \mathbf{r} \in \cap_i, \quad \forall i = 1, n_{\cap}. \end{cases} \quad (\text{A5})$$

371 Here,  $\delta_{ij}$  is the Kronecker symbol. These functions are perfectly defined, as being the unique solution of a Dirichlet  
372 Neumann problem. We can decompose the pressure along the  $j^{\text{th}}$  intersection:

$$p_{\cap_j}(x) = \sum_{n=1}^{\infty} P_j^n \Phi_j^n(x), \quad (\text{A6})$$

373 and we define  $p_{\cap}(\mathbf{r})$  as the solution of the Laplace equation, without source term but with the imposed profiles at the  
374 intersections. We have:

$$p_{\cap}(\mathbf{r}) = \sum_{j \in J_I} \sum_{n=1}^{\infty} P_j^n \hat{P}_j^n(\mathbf{r}). \quad (\text{A7})$$

375 We consider now the complete Laplace limit problem (A1). We suppose that the pressures profiles at all the existing  
376 intersections are known:  $P_j(\mathbf{r})$ . Using the linearity of the Laplace equation, and the boundary conditions, we showed

377 that:

$$p(\mathbf{r}) = \sum_{j \in J_I} \sum_{n=1}^{\infty} P_j^n \hat{P}_j^n(\mathbf{r}) + \int_{\Omega_I} d^2 \mathbf{r}' B(\mathbf{r}, \mathbf{r}') \times g_I(\mathbf{r}'). \quad (\text{A8})$$

378 Here the Green's function  $B(\mathbf{r}, \mathbf{r}')$  is an elementary solution of the Laplace problem, with a source term  $\delta(\mathbf{r} - \mathbf{r}')$ :

$$\forall I = 1, \dots, N, \quad \nabla_{\mathbf{r}} \cdot (k_I \nabla_{\mathbf{r}} B(\mathbf{r}, \mathbf{r}')) = \delta(\mathbf{r} - \mathbf{r}'). \quad (\text{A9})$$

379 to be solved with the following boundary conditions:

$$\begin{aligned} k_I \nabla_{\mathbf{r}} B(\mathbf{r}, \mathbf{r}') \cdot \mathbf{n} &= 0 \quad \text{for } \mathbf{r} \in \partial \Omega_I, \\ B(\mathbf{r}, \mathbf{r}') &= 0 \quad \text{if } \mathbf{r} \in \cap_i, \quad \forall i = 1, n_{\cap}. \end{aligned}$$

380 One must remember that it is a 2D Green's function, because the working space is the space of the fracture. This is  
381 the general form of the solution with source term, but we still need relations to determine the set of  $P_j^n$  values. This  
382 will be done by using the boundary condition (A2) in next subsection.

383 In order to get equations allowing to determine the unknowns  $P_i^m$ , we use the boundary condition (A2), conveniently  
384 projected on the basis function  $\Phi_i^m(x)$ . The projection gives the following relation:  $\forall i = 1, \dots, n_{\cap}, \quad \forall m = 1, \dots, \infty$ ,

$$\begin{aligned} \int_{\cap_i} dx \mathbf{n}_{\cap_I J I \ell} \cdot k_I(\mathbf{r}(x)) [\nabla_I p(\mathbf{r}_{\cap_I J}(x))_{\ell} - \nabla_I p(\mathbf{r}_{\cap_I J}(x))_{\mathbf{r}}] \times \Phi_i^m(x) \\ + \int_{\cap_i} dx \mathbf{n}_{\cap_I J J \ell} \cdot k_J(\mathbf{r}(x)) [\nabla_J p(\mathbf{r}_{\cap_I J}(x))_{\ell} - \nabla_J p(\mathbf{r}_{\cap_I J}(x))_{\mathbf{r}}] \times \Phi_i^m(x) = 0. \end{aligned} \quad (\text{A10})$$

385 This allows us to get an infinite set of relations, by inserting (A8) in the projection of the boundary conditions (A10)  
386 :  $\forall i, \dots, m$ ,

$$\sum_{j \in J(i)} \sum_{n=1}^{\infty} T_{ij}^{mn} \times P_j^n + \int_{\Omega_I} d^2 \mathbf{r}' B_i^m(\mathbf{r}') \times g_I(\mathbf{r}') + \int_{\Omega_{I(i)}} d^2 \mathbf{r}' B_i^m(\mathbf{r}') \times g_{I(i)}(\mathbf{r}') = 0. \quad (\text{A11})$$

387 or, equivalently, introducing  $B_i^m = - \int_{\Omega_I} d^2 \mathbf{r}' B_i^m(\mathbf{r}') \times g_I(\mathbf{r}') - \int_{\Omega_{I(i)}} d^2 \mathbf{r}' B_i^m(\mathbf{r}') \times g_{I(i)}(\mathbf{r}')$ :

$$\sum_{j \in J(i)} \sum_{n=1}^{\infty} T_{ij}^{mn} \times P_j^n = B_i^m, \quad (\text{A12})$$

388 In order to emphasize the overall linearity of the problem, we have introduced the following quantities  $T_{ij}^{nm}$  and  $B_i^m$

389 as:

$$T_{ij}^{mn} = \int_{\Omega_i} dx \mathbf{n}_{\Omega_{IJ}I\ell} \cdot k_I(\mathbf{r}(x)) [\nabla_I \hat{P}_j^n(\mathbf{r}(x))_\ell - \nabla_I \hat{P}_j^n(\mathbf{r}(x))_r] \times \Phi_i^m(x), \quad (\text{A13})$$

$$B_i^m(\mathbf{r}') = \int_{\Omega_i} dx \mathbf{n}_{\Omega_{IJ}I\ell} \cdot k_I(\mathbf{r}(x)) [\nabla_I B(\mathbf{r}(x), \mathbf{r}')_\ell - \nabla_I B(\mathbf{r}(x), \mathbf{r}')_r] \times \Phi_i^m(x). \quad (\text{A14})$$

390 It was shown in [1], and the proof is presented in the appendix C that  $T_{ij}^{nm}$  and  $B_i^m(\mathbf{r}')$  may be written under a much

391 more simple and explicit form:

$$T_{ij}^{mn} = \int_{\Omega_I} d^2 \mathbf{r} k_I(\mathbf{r}) \nabla_I \hat{P}_i^m(\mathbf{r}) \cdot \nabla_I \hat{P}_j^n(\mathbf{r}), \quad (\text{A15})$$

$$B_i^m(\mathbf{r}') = \hat{P}_i^m(\mathbf{r}'). \quad (\text{A16})$$

392 The notation  $\sum'$  means that the summation must be performed over both fractures involved by the  $i^{\text{th}}$  intersection  
 393 of the  $I^{\text{th}}$  fracture. Here, the notation  $I(i)$  denotes that we are considering the moment of the solution over the  $i^{\text{th}}$   
 394 intersection, between the  $I^{\text{th}}$  fracture, and the  $I(i)^{\text{th}}$  intersection. It is this summation over all the involved fractures  
 395 that permits to ensure mass conservation at the intersections. In order to simplify the presentation, we did not  
 396 reintroduce the labels of I and J th fractures. In practice, one will truncate the order  $n$  of the approximation by  
 397 restricting  $m, n \leq n_0$ . At the end of the process, we will have to solve a linear system of  $N_\cap \times n_0$  equations. To the  
 398 lowest order approximation  $n_0 = 1$ , will correspond  $N_\cap$  equations to be solved. This corresponds well to our initial  
 399 program, this approximation will be studied in more details in Section 7.

400 The algebraic form (A15) permits to check by direct inspection that we have the general symmetry relation:

$$T_{ij}^{mn} = T_{ji}^{nm},$$

401 for all labels  $i, j, m$  and  $n$ .

402 It can be checked by inspection of this formula that the matrix  $T_{ij}^{11}$  is symmetric, positive. It is not definite because

403 we have the general relation:

$$\sum_j T_{ij}^{11} = 0. \quad (\text{A17})$$

404 This equality can be derived by noticing that we have the general sum rule:

$$P(\mathbf{r}) = \sum_{j=1, n \in I} \hat{P}_j^1(\mathbf{r}) = 1. \quad (\text{A18})$$

## 405 APPENDIX B: PROJECTION FORMALISM QUASI STEADY STATE CASE

406 We come back to the full transient diffusion problem 3 on the fracture network. Our present goal is to build an  
 407 approximation scheme valid for time scales greater to a typical diffusion time over one fracture. For a typical fracture  
 408  $I$  of permeability  $k_I$  and of size  $L_I$ , this time scale is of order  $L_I^2/D_I$ , here the diffusion coefficient is given by  
 409  $D_I = k_I/\varphi\mu c_t$ . Let  $p(\mathbf{r}, t)$  be the solution of the full diffusion problem. We write  $p(\mathbf{r}, t)$  under the following form:

$$p(\mathbf{r}, t) = \delta p(\mathbf{r}, t) + \sum_{j \in J_I} \sum_{n=1}^{\infty} P_j^n(t) \hat{P}_j^n(\mathbf{r}) + \int_{\Omega_I} d^2\mathbf{r}' B(\mathbf{r}, \mathbf{r}') \times g_I(\mathbf{r}').$$

410 Here, the  $P_j^n(t)$  are assumed to be “slowly varying” if compared to typical diffusion time over one fracture. The  
 411 steady state assumption assumes that the residual term  $\delta p(\mathbf{r}, t)$  obeys a steady state equation. It means physically  
 412 that internal degrees of freedom inside a fracture are driven by the value of the potential at the intersections.

413  $\delta p(\mathbf{r}, t)$  obeys the following equation:

$$\varphi\mu c_t \frac{\partial \delta p(\mathbf{r}, t)}{\partial t} = \nabla \cdot (k_I \nabla \delta p(\mathbf{r}, t)) - \varphi\mu c_t \sum_{j \in J_I} \sum_{n=1}^{\infty} \dot{P}_j^n(t) \hat{P}_j^n(\mathbf{r}), \quad \text{with} \quad \dot{P}_j^n(t) = \frac{dP_j^n(t)}{dt},$$

414 with an additional condition:

$$\delta p(\mathbf{r}, t) = 0 \quad \text{if} \quad \mathbf{r} \in \cup \cap_i.$$

415 The definition of  $\hat{P}_j^n(\mathbf{r})$  explains the overall simplification. Now, we can use the pseudo steady state assumption  
 416 to drop the partial time derivative in the LHS. It means physically that the pressure inside a given fracture follows a

417 steady state problem with a source term given by the term  $\left(\varphi\mu c_t \sum_{j \in J_I} \sum_{n=1}^{\infty} \dot{P}_j^n(t) \hat{P}_j^n(\mathbf{r})\right)$ . We get:

$$\nabla \cdot (k_I \nabla \delta p(\mathbf{r}, t)) = \varphi\mu c_t \sum_{j \in J_I} \sum_{n=1}^{\infty} \dot{P}_j^n(t) \hat{P}_j^n(\mathbf{r}).$$

418 In this expression, the term  $\left(\varphi\mu c_t \sum_{j \in J_I} \sum_{n=1}^{\infty} \dot{P}_j^n(t) \hat{P}_j^n(\mathbf{r})\right)$  is a surface source term that appears due to the changing  
419 forcing term at the intersections. It specifies the form of the  $g_I(\mathbf{r})$ . Using the general solution with source term (A8),  
420 we get thus the following solution:

$$p(\mathbf{r}, t) = \sum_{j \in J_I} \sum_{n=1}^{\infty} P_j^n(t) \hat{P}_j^n(\mathbf{r}) + \int_{\Omega_I} d^2\mathbf{r}' B(\mathbf{r}, \mathbf{r}') \times g_I(\mathbf{r}') + \int_{\Omega_I} d^2\mathbf{r}' B(\mathbf{r}, \mathbf{r}') \times \sum_{j \in J_I} \sum_{n=1}^{\infty} \varphi\mu c_t \dot{P}_j^n(t) \hat{P}_j^n(\mathbf{r}'). \quad (\text{B1})$$

421 Using thus the boundary condition (A2) that remains fulfilled also in transient cases, we can follow the same analysis  
422 than in the steady state case with source term to get equations relating the pressure and its time derivatives. We  
423 obtain:

$$\begin{aligned} \forall i, m, \quad & \sum_{j \in J(i)} \sum_{n=1}^{\infty} T_{ij}^{mn} \times P_j^n + \int_{\Omega_I} d^2\mathbf{r} B_i^m(\mathbf{r}) \times g_I(\mathbf{r}') + \int_{\Omega_I} d^2\mathbf{r} B_i^m(\mathbf{r}) \times \sum_{j \in J(i)} \sum_{n=1}^{\infty} \varphi\mu c_t \dot{P}_j^n(t) \hat{P}_j^n(\mathbf{r}) \\ & + \int_{\Omega_{I(i)}} d^2\mathbf{r} B_i^m(\mathbf{r}) \times g_I(\mathbf{r}') + \int_{\Omega_{I(i)}} d^2\mathbf{r} B_i^m(\mathbf{r}) \times \sum_{j \in J(i)} \sum_{n=1}^{\infty} \varphi\mu c_t \dot{P}_j^n(t) \hat{P}_j^n(\mathbf{r}) = 0. \quad (\text{B2}) \end{aligned}$$

424 Let us introduce the “mass matrix”  $K_{ij}^{mn}$  by means of the definition:

$$K_{ij}^{mn} = \int_{\Omega_I} d^2\mathbf{r} B_i^m(\mathbf{r}) \times \varphi\mu c_t \hat{P}_j^n(\mathbf{r}) = \varphi\mu c_t \int_{\Omega_I} d^2\mathbf{r} \hat{P}_i^m(\mathbf{r}) \hat{P}_j^n(\mathbf{r}). \quad (\text{B3})$$

425 Here, we have used directly the equality (A16). The set of equations can be rewritten under a more synthetic form:

$$\forall i, m, \quad \sum_{j \in J(i)} \sum_{n=1}^{\infty} K_{ij}^{mn} \times \frac{dP_j^n(t)}{dt} = \sum_{j \in J(i)} \sum_{n=1}^{\infty} T_{ij}^{mn} \times P_j^n + B_i^m. \quad (\text{B4})$$

426 Summarizing the mass and transmissibility matrices, we get remarkable expressions involving surfaces integrals of

427 the base solutions:

$$T_{ij}^{mn} = \int_{\Omega_I} d^2\mathbf{r} k_I(\mathbf{r}) \nabla_I \hat{P}_i^m(\mathbf{r}) \cdot \nabla_I \hat{P}_j^n(\mathbf{r}), \quad (\text{B5})$$

$$K_{ij}^{mn} = \varphi \mu c_t \int_{\Omega_I} d^2\mathbf{r} \hat{P}_i^m(\mathbf{r}) \hat{P}_j^n(\mathbf{r}). \quad (\text{B6})$$

428  $T_{ij}^{mn}$  and  $K_{ij}^{mn}$  appear as “scalar products” of the basic solutions or of their gradients. These expressions appear also  
 429 in a finite element context [43]. The symmetry and positiveness of the matrices  $\mathbf{K}$  and  $\mathbf{T}$  can be checked by direct  
 430 inspection:

$$T_{ij}^{mn} = T_{ji}^{nm}, \quad (\text{B7})$$

$$K_{ij}^{mn} = K_{ji}^{nm}, \quad (\text{B8})$$

431 for all labels  $i, j, m$  and  $n$ . Direct numerical methods can be set up to determine the transmissivity  $T_{ij}^{mn}$  and the  
 432 mass matrix  $K_{ij}^{mn}$ . Each Laplace boundary value problem (A5) can be solved on each fracture independently of the  
 433 others once the intersection segments have been determined. This means that internal degrees of freedom between  
 434 different fractures are not directly coupled. This is quite natural, as all the information must be carried by the  
 435 intersections. The boundary value problem (A5) can be solved using for example a finite element code by meshing  
 436 only the  $I^{th}$  fracture, once for all  $i, j, m$  and  $n$ , plus a Laplace equation solver. High values of  $m$  and  $n$  will probably  
 437 need highly refined meshes, corresponding to having a high level of details. The same procedure must evidently  
 438 be repeated for every fracture, leading to a numerical cost proportional to twice the total number of intersections.  
 439 Finding a method to control the accuracy of the method as a function of  $m$  and  $n$  would be of theoretical interest.  
 440 Fast evaluations methods of  $\mathbf{K}$  and  $\mathbf{T}$  remain an open area of work followed by Khvoenkova and Delorme [42]. The  
 441 similar approach followed in  $2D$ , with fracture intersections that degenerate as single points is exact, and corresponds  
 442 to a so called resistor/network model developed by [31].

## APPENDIX C: DERIVATION OF EQ. (A15) AND EQ. (A16)

443

444 We want to show that:

$$T_{ij}^{mn} = \int_{\Omega_I} d^2\mathbf{r} k_I(\mathbf{r}) \nabla_I \hat{P}_i^m(\mathbf{r}) \cdot \nabla_I \hat{P}_j^n(\mathbf{r}), \quad (\text{C1})$$

$$B_i^m(\mathbf{r}') = \hat{P}_i^m(\mathbf{r}'). \quad (\text{C2})$$

445 We start from the definitions:

$$\begin{aligned} T_{ij}^{mn} &= \int_{\cap_i} dx \mathbf{n}_{\cap_I J I \ell} \cdot k_I(\mathbf{r}(x)) [\nabla_I \hat{P}_j^n(\mathbf{r}(x))_\ell - \nabla_I \hat{P}_j^n(\mathbf{r}(x))_r] \times \Phi_i^m(x), \\ B_i^m(\mathbf{r}') &= \int_{\cap_i} dx \mathbf{n}_{\cap_I J I \ell} \cdot k_I(\mathbf{r}(x)) [\nabla_I B(\mathbf{r}(x), \mathbf{r}')_\ell - \nabla_I B(\mathbf{r}(x), \mathbf{r}')_r] \times \Phi_i^m(x), \end{aligned} \quad (\text{C3})$$

446 with  $P_i^m(\mathbf{r})$  which is solution of the following boundary value problem:

$$\begin{cases} \nabla_I \cdot (k_I \nabla \hat{P}_i^m(\mathbf{r})) = 0, \\ k_I \nabla \hat{P}_i^m(\mathbf{r}) \cdot \mathbf{n} = 0 \quad \text{on} \quad \partial\Omega_I, \\ \hat{P}_i^m(\mathbf{r}) = \delta_{ij} \times \Phi_i^m(\mathbf{r}) \quad \text{if} \quad \mathbf{r} \in \cap_i, \quad \forall j = 1, n_\cap. \end{cases}$$

447 These equalities may be derived by remarking that  $T_{ij}^{mn}$  and  $B_i^m(\mathbf{r}')$  can be rewritten under a slightly different form:

$$\begin{aligned} T_{ij}^{mn} &= \int_{\cap_i} dx \mathbf{n} \cdot k_I(\mathbf{r}(x)) [\nabla_I \hat{P}_j^n(\mathbf{r}(x)) - \nabla_I \hat{P}_j^n(\mathbf{r}(x))_r] \times \Phi_i^m(x) \\ &= \int_{\cap_i} dx \mathbf{n} \cdot k_I(\mathbf{r}(x)) \nabla_I \hat{P}_j^n(\mathbf{r}(x)) \times \hat{P}_i^m(\mathbf{r}(x)) \\ &= \int_{\cup \cap_k \cup \partial\Omega_I} dr \mathbf{n} \cdot k_I(\mathbf{r}(x)) \nabla_I \hat{P}_j^n(\mathbf{r}(x)) \times \hat{P}_i^m(\mathbf{r}(x)) \\ B_i^m(\mathbf{r}') &= \int_{\cup \cap_k \cup \partial\Omega_I} dx \mathbf{n} \cdot k_I(\mathbf{r}(x)) \nabla_I B(\mathbf{r}(x), \mathbf{r}') \times \hat{P}_i^m(\mathbf{r}(x)). \end{aligned}$$

448 In order to understand the second and fourth equalities, the reader must imagine that the intersection contour is a  
 449 closed 2D contour of small thickness allowing to replace the contribution of left and right fluxes on the two sides of  
 450 the intersection by a contour integral that allows to use Green's theorem. We did not change the notations in order  
 451 to simplify the presentation. In present form, the boundary integrals are extended on all the frontiers associated with  
 452 the  $I^{th}$  fracture, so we can use Green's theorem in order to transform the contour integral on a surface integral over

453 the fracture domain. We obtain:

$$T_{ij}^{mn} = \int_{\Omega_I} d^2\mathbf{r} \nabla \cdot [k_I(\mathbf{r}) \nabla_I \hat{P}_j^n(\mathbf{r}) \times \hat{P}_i^m(\mathbf{r})],$$

454 from which the desired identity follows, using once again the local equation obeyed by  $\hat{P}_j^n(\mathbf{r})$ :

$$T_{ij}^{mn} = \int_{\Omega_I} d^2\mathbf{r} k_I(\mathbf{r}) \nabla_I \hat{P}_j^n(\mathbf{r}) \cdot \nabla \hat{P}_i^m(\mathbf{r}).$$

455 For  $B_i^m(\mathbf{r}')$  we need some additional manipulations in the same style:

$$\begin{aligned} B_i^m(\mathbf{r}') &= \int_{\cup \cap_k \cup \partial \Omega_I} dx \mathbf{n} \cdot k_I(\mathbf{r}) \nabla_I B(\mathbf{r}(x), \mathbf{r}') \times \hat{P}_i^m(\mathbf{r}(x)) \\ &= \int_{\Omega_I} d^2\mathbf{r} \nabla \cdot [k_I(\mathbf{r}) \nabla_I B(\mathbf{r}, \mathbf{r}') \times \hat{P}_i^m(\mathbf{r})]. \end{aligned} \quad (\text{C4})$$

456 Using the equation defining  $B(\mathbf{r}, \mathbf{r}')$ , we obtain:

$$B_i^m(\mathbf{r}') = \hat{P}_i^m(\mathbf{r}') + \int_{\Omega_I} d^2\mathbf{r} k_I(\mathbf{r}) \nabla_I B(\mathbf{r}, \mathbf{r}') \cdot \nabla \hat{P}_i^m(\mathbf{r}).$$

457 The second term of the RHS may be written under a more explicit form:

$$\begin{aligned} \int_{\Omega_I} d^2\mathbf{r} k_I(\mathbf{r}) \nabla_I B(\mathbf{r}, \mathbf{r}') \cdot \nabla \hat{P}_i^m(\mathbf{r}) &= \int_{\Omega_I} d^2\mathbf{r} k_I(\mathbf{r}) \nabla_I B(\mathbf{r}, \mathbf{r}') \cdot \nabla \hat{P}_i^m(\mathbf{r}) \\ &\quad + \int_{\Omega_I} d^2\mathbf{r} B(\mathbf{r}, \mathbf{r}') \nabla_I \cdot [k_I(\mathbf{r}) \nabla \hat{P}_i^m(\mathbf{r})] \\ &= \int_{\Omega_I} d^2\mathbf{r} \nabla_I \cdot [k_I(\mathbf{r}) B(\mathbf{r}, \mathbf{r}') \nabla \hat{P}_i^m(\mathbf{r})] \\ &= \int_{\cup \cap_k \cup \partial \Omega_I} dr k_I(\mathbf{r}) B(\mathbf{r}, \mathbf{r}') \times \nabla_I \hat{P}_i^m(\mathbf{r}) \cdot \mathbf{n} \end{aligned}$$

458 But the last expression is equal to zero, thanks to the boundary conditions on  $B(\mathbf{r}, \mathbf{r}')$  and  $k_I(\mathbf{r}) \nabla_I \hat{P}_i^m(\mathbf{r}) \cdot \mathbf{n}$  on

459  $\cup \cap_k \cup \partial \Omega_I$ .

$$\int_{\cup \cap_k \cup \partial \Omega_I} dr k_I(\mathbf{r}) B(\mathbf{r}, \mathbf{r}') \times \nabla_I \hat{P}_i^m(\mathbf{r}) \cdot \mathbf{n} = 0.$$

460 This provides the announced result.



- 
- 461 [1] B. Noetinger, N. Jarrige A quasi steady state method for solving transient Darcy flow in complex 3D fractured  
462 networks Journal of Computational Physics, Volume 231, Issue 1, 1 January 2012, Pages 23-38, ISSN 0021-9991,  
463 10.1016/j.jcp.2011.08.015.
- 464 [2] G.I. Barenblatt, I.P. Zheltov, and I.N. Kochina. Basic concepts in the theory of seepage of homogeneous liquids in fissured  
465 rocks. Journal of Applied Mathematics and Mechanics, 24(5):1286–1303, 1960
- 466 [3] J.C. Sabathier, B.J. Bourbiaux, MC Cacas, and S. Sarda. A new approach of fractured reservoirs. SPE Paper #39825  
467 International Petroleum Conference and Exhibition of Mexico, 1998.
- 468 [4] B.J. Bourbiaux, S. Granet, P. Landereau, B. Noetinger, S. Sarda, J.C. Sabathier, Scaling Up Matrix-Fracture Transfers  
469 in Dual-Porosity Models: Theory and Application SPE Paper # 56557 SPE Annual Technical Conference and Exhibition,  
470 3-6 October 1999, Houston, Texas
- 471 [5] P.M. Adler and J.F. Thovert. *Fractures and Fracture Networks*. Kluwer, Dordrecht, 1999.
- 472 [6] S. Sarda, L. Jeannin, R. Basquet, and B.J. Bourbiaux. Hydraulic characterization of fractured reservoirs: Simulation on  
473 discrete fracture models. SPE Paper #73300 , Reservoir Evaluation & Engineering, Vol 5(2) 154-162, April 2002.
- 474 [7] S.P. Neuman. Trends, prospects and challenges in quantifying flow and transport through fractured rocks. Hydrogeology  
475 Journal, 13(1):124–147, 2005.
- 476 [8] B.J. Bourbiaux Fractured Reservoir Simulation: a Challenging and Rewarding Issue Oil Gas Sci. Technol. - Rev. IFP 65  
477 2 (2010) 227-238 DOI: 10.2516/ogst/2009063
- 478 [9] P. Lemonnier, B. Bourbiaux Simulation of Naturally Fractured Reservoirs. State of the Art - Part 1 - Physical Mechanisms  
479 and Simulator Formulation. Oil Gas Sci. Technol.- Rev. IFP 65 2 (2010) 239-262 DOI: 10.2516/ogst/2009066
- 480 [10] P. Lemonnier, B. Bourbiaux Simulation of Naturally Fractured Reservoirs. State of the Art - Part 2 - Matrix-Fracture  
481 Transfers and Typical Features of Numerical Studies Oil Gas Sci. Technol. - Rev. IFP 65 2 (2010) 263-286 DOI:  
482 10.2516/ogst/2009067
- 483 [11] T. Arbogast, J. Douglas Jr, and U. Hornung. Derivation of the double-porosity model of single-phase flow via homoge-  
484 nization theory. SIAM J. Math. Anal., 21(4):823–836, July 1990.
- 485 [12] M. Panfilov. Averaged model-type transition in flows through multiple heterogeneous porous media. C.R. Acad. Sci.  
486 Paris, 318(II):1437–1443, 1994.
- 487 [13] P. Royer, J.L. Auriault, and C. Boutin. Macroscopic modeling of double-porosity reservoirs. Journal of Petroleum Science  
488 and Engineering, 16(4):187–202, 1996.
- 489 [14] R.E. Showalter. In *Homogenization and Porous Media*, volume 6 of Interdisciplinary Applied Mathematics Series, chapter  
490 Micro-structure Models of Porous Media. Springer, New York, 1997.
- 491 [15] M. Quintard and S. Whitaker. Transport in chemically and mechanically heterogeneous porous media I: Theoretical  
492 development of region-averaged equations for slightly compressible single-phase flow. Advances in Water Resources,  
493 19(1):29-47, 1996.
- 494 [16] M. Quintard and S. Whitaker. Transport in chemically and mechanically heterogeneous porous media ii: Comparison with  
495 numerical experiments for slightly compressible single-phase flow. Advances in Water Resources, 19(1):49-60, 1996.
- 496 [17] P. Landereau, B. Noetinger, and M. Quintard. Quasi-steady two-equation models for diffusive transport in fractured porous  
497 media: large-scale properties for densely fractured systems. Advances in Water Resources, 24 (8):863-876, 2001.
- 498 [18] J.F. McCarthy. Effective permeability of sandstone-shale reservoirs by a random walk method. J. Phys. A: Math. Gen.,  
499 23:445–451, 1990.
- 500 [19] J.F. McCarthy. Continuous-time random walks on random media. J. Phys. A: Math. Gen., 26:2495–2503, 1993.
- 501 [20] B. Noetinger and T. Estebenet. Up scaling of fractured porous media using a continuous time random walk method.  
502 Transport in Porous Media, 39:315–337, 2000.
- 503 [21] B. Noetinger, T. Estebenet, and M. Quintard. Up scaling of fractured media: Equivalence between the large scale averaging  
504 theory and the continuous time random walk method. Transport in Porous Media, 43:581–596, 2001.
- 505 [22] B. Noetinger, T. Estebenet, and P. Landereau. A direct determination of the transient exchange term of fractured media  
506 using a continuous time random walk method. Transport in Porous Media, 44:539–557, 2001.
- 507 [23] A de Swaan Analytic solutions for determining naturally fractured reservoir properties by well testing SPE Journal, 5 4  
508 117–22 1976
- 509 [24] A de Swaan Influence of shape and skin of matrix-rock blocks on pressure transients in fractured reservoirs SPE formation  
510 evaluation, 5 4 344–352 1990
- 511 [25] A De Swann. and Ramirez-Villa, M. Functions of flow from porous rock blocks. Journal of Petroleum Science and  
512 Engineering, vol. 9, no 1, p. 39-48. 1993
- 513 [26] F.Daviau Interprétation des essais de puits : les méthodes nouvelles ed Technip, Paris 1986
- 514 [27] L. De Arcangelis, J. Koplik, S. Redner, and D. Wilkinson. Hydrodynamic Dispersion in Network Models of Porous Media.  
515 Phys. Rev. Lett., 57:986–999, 1986.
- 516 [28] J. Koplik, S. Redner, and D. Wilkinson. Transport and dispersion in random networks with percolation disorder. Physical  
517 Review A, 37:2619–2636, 1988.
- 518 [29] B. Berkowitz and I. Balberg. Percolation theory and its application to groundwater hydrology. Water Res. Res., 29(4):775–  
519 794, 1993.
- 520 [30] J. Chang and Y.C. Yortsos Pressure transient analysis of fractal reservoirs. SPE Paper # 18170, SPE Form. Eval., Vol  
521 5(1)pages 31–38, 1990.

- 522 [31] J.A. Acuna and Y.C. Yortsos. Application of fractal geometry to the study of networks of fractures and their pressure  
523 transient. *Water Res. Res.*, 31 3:527–540, 1995.
- 524 [32] R.W. Zimmerman, G. Chen, T. Hadgu, and G.S. Bodvarsson. A numerical dual-porosity model with semi-analytical  
525 treatment of fracture/matrix flow. *Water Res. Res.*, 29:2127–37, 1993.
- 526 [33] V.V. Mourzenko, J-F. Thovert, and P.M. Adler. Geometry of simulated fractures. *Physical Review E*, 53(6), 1996.
- 527 [34] J. Douglas, F. Pereira, and L.M. Yeh. A parallelizable method for two-phase flows in naturally-fractured reservoirs. *Comput.*  
528 *Geosci.*, 1(3-4):333–368, 1997.
- 529 [35] S. Granet, P. Fabrie, P. Lemonnier, and M. Quintard. A two-phase flow simulation of a fractured reservoir using a new  
530 fissure element method. *Journal of Petroleum Science and Engineering*, 32(1):35–52, 2001.
- 531 [36] A. Lange, R. Basquet, B. Bourbiaux, et al. Hydraulic characterization of faults and fractures using a dual medium discrete  
532 fracture network simulator. SPE Paper # 88675 In 10th International Petroleum Exhibition and Conference, Abu Dhabi.  
533 SPE, 2002.
- 534 [37] T.N. Narasimhan and K. Pruess. MINC: An approach for analyzing transport in strongly heterogeneous systems. in  
535 *Groundwater Flow and Quality Modeling*. D. Reidel Publishing Co. Boston. 1988. p 375-391, 4 fig, 21 ref., 1988.
- 536 [38] I.I. Bogdanov, V.V. Mourzenko, J.F. Thovert, and P.M. Adler. Pressure drawdown well tests in fractured porous media.  
537 *Water Res. Res.*, 39(1):1021, 2003a.
- 538 [39] A. Fournon, C. Grenier, F. Delay, E. Mouche, and H. Benabderrahmane. Smearred fractures: a promising approach to model  
539 transfers in fractured media. *Developments in Water Science*, 55:1003–1014, 2004.
- 540 [40] G. Pichot, J. Erhel and J. R. de Dreuzy, A mixed hybrid Mortar method for solving flow in discrete fracture networks,  
541 *Applicable Analysis An International Journal*, 89 Issue 10, 1629, doi:10.1080/00036811.2010.495333
- 542 [41] Y.S. Wu. Numerical simulation of single-phase and multiphase non-Darcy flow in porous and fractured reservoirs. *Transport*  
543 *in porous media*, 49(2):209–240, 2002.
- 544 [42] N. Khvoenkova and M. Delorme. An Optimal Method to Model Transient Flows in 3D Discrete Fracture Network. IAMG  
545 conference 2011 Salzburg, Austria, 2011.
- 546 [43] Y. Efendiev, J. Galvis, and X.H. Wu. Multiscale finite element methods for high-contrast problems using local spectral  
547 basis functions. *J. Comput. Phys.*, 230 2011 937–955.
- 548 [44] I.I. Bogdanov, V.V. Mourzenko, J.F. Thovert, and P.M. Adler. Effective permeability of fractured porous media in steady  
549 state flow. *Water Resour. Res.*, 39(1):1023, 2003b.
- 550 [45] H. Stehfest. Algorithm 368: Numerical inversion of laplace transforms [d5]. *Commun. ACM*, 13:47-49, January 1970.

